JTEP Jurnal Keteknikan Pertanian,
Vol. 13 No. 4, p 529-545, 2025
P-ISSN 2407-0475 E-ISSN 2338-8439

Available online:
http://journal.ipb.ac.id/index.php/jtep
DOI: 10.19028/jtep.013.4.329-545

Analysis of Temperature and Airflow Distribution during Carrot Drying Using a Tray Dryer Based on CFD Simulation

Renny Eka Putri[1*], Annisa Octaviani Putri[1], Muhammad Iqbal Abdi Lubis[1]

[1]Department of Agricultural and Biosystem Engineering, Faculty of Agricultural Technology, Andalas University, Limau Manis, Pauh, Padang, Indonesia.

*Corresponding author, email: rennyekaputri@unand.ac.id

Article Info

Submitted: 28 July 2025
Revised: 9 October 2025
Accepted: 26 November 2025
Available online: 4 Desember 2025
Published: December 2025

Keywords:
ANSYS Fluent, Drying Process, Heat Transfer, Temperature, Thermodynamics

How to cite:
Putri, R. K., Putri, A. O., Lubis, M. I. A (2025). Analysis of Temperature and Airflow Distribution during Carrot Drying Using a Tray Dryer Based on CFD Simulation. Jurnal Keteknikan Pertanian, 13(4): 529-542. https://doi.org/*10.19028/jtep.013.4.529-545.*

Abstract

Carrot (Daucus carota L.) is a highly nutritious vegetable that is prone to spoilage due to its high moisture content. Drying is an effective method to extend its shelf life, with the tray dryer being one of the commonly used technologies. However, the efficiency of the drying process greatly depends on the uniformity of temperature and airflow distribution within the drying chamber. This study aims to analyze the distribution of temperature and airflow inside a tray dryer using Computational Fluid Dynamics (CFD) during the drying of carrots. Simulations were conducted at three different temperatures (50°C, 60°C, and 70°C) and two air velocities (2 m/s and 3 m/s) using SolidWorks, ANSYS Fluent, and Origin software. The simulation results showed that both temperature and airflow were unevenly distributed, particularly in the middle and upper sections of the dryer. This non-uniformity can lead to inconsistent drying and reduced product quality. Validation was carried out by comparing simulation results with experimental measurements using relative error analysis. The error values obtained ranged from 1.41% to 3.82% for temperature and 0.5% to 2.41% for air velocity, all below 4%. These results indicate that the CFD model is sufficiently accurate and can be applied to support the design and optimization of more efficient drying equipment.

Doi: https://doi.org/10.19028/jtep.013.4.529-545

1. ntroduction

Carrot (Daucus carota L.) is one of the root vegetables with high economic value in Indonesia. This vegetable is widely found in various regions and can grow throughout the year, in both the rainy and dry seasons. According to the Central Statistics Agency of West Sumatra Province, in 2022, carrot production in West Sumatra reached 25,282 thousand tons, an increase of 0.69% from the 25,457 thousand tons produced in 2021. The highest carrot production each year is concentrated in Solok, Tanah Datar, and Agam Regencies (Central Statistics Agency of West Sumatra Province, 2020). Carrot is one of the agricultural commodities rich in nutrients, particularly vitamin A, fiber, and antioxidants. In addition, it has a high moisture content, making it highly perishable and prone to spoilage (Histifarina et al., 2004).

JTEP Jurnal Keteknikan Pertanian,
Vol. 13 No. 4, p 529-545, 2025
P-ISSN 2407-0475 E-ISSN 2338-8439
Available online:
http://journal.ipb.ac.id/index.php/jtep
DOI: 10.19028/jtep.013.4.329-545

Drying is one of the most important processes in agricultural product processing, particularly for extending the shelf life and maintaining product quality (Triyastuti et al., 2018). This process aims to remove moisture from food materials to prevent spoilage caused by microorganisms and oxidation (Al-Kindi et al., 2015). Carrot (Daucus carota L.), as a vegetable rich in nutrients, is often processed into dried products to facilitate storage and distribution. However, effective carrot drying requires a deep understanding of hot air flow and heat transfer during the drying process.

A tray dryer, also known as a rack-type dryer, is a commonly used device for drying processes, particularly for agricultural products. Drying using a tray dryer is often chosen because of its efficiency and ability to produce high-quality dried products. The tray dryer operates by circulating hot air around the material being dried, and the distribution and velocity of the airflow significantly influence the drying rate. Therefore, airflow analysis within the tray dryer is crucial for optimizing the drying process (Kereh et al., 2022). In general, the greater the temperature difference between the heating medium and the food material, and the faster the airflow movement during the drying process, the faster the heat transfer occurs, the more rapidly water evaporates, the more quickly the material dries, and the more significantly the drying efficiency improves (Saidi & Wulandari, 2019).

In recent years, the use of Computational Fluid Dynamics (CFD) has increased in the study of drying processes. CFD is a numerical technique used to model and analyze fluid flow, heat transfer, transport phenomena, and chemical reactions in systems, including airflow within tray dryers (Tayyeb et al., 2013). CFD enables accurate simulations of fluid and gas flows, providing insights into flow patterns, temperature distributions, and drying effectiveness. CFD modelling facilitates the visualization of airflow within tray dryers and helps evaluate key parameters that influence the drying process, such as air temperature and airflow velocity (Daza-Gómez et al., 2022).

One study conducted by Anwar and Panggabean (2019) analyzed the temperature and airflow distribution within a rack-type dryer used for drying temulawak chips using a CFD simulation. The results indicated that CFD simulations successfully validated the temperature and airflow distribution within the dryer, both in empty and loaded conditions, with average temperature validation errors of 1.06% and 2.62%, respectively. Thus, the simulation was considered valid for improving the drying process. Another study by Histifarina et al. (2004) on carrot drying found that a 32-hour drying time combined with a drying temperature of 50℃ produced the best-dried carrot with a moisture content of 9.15%. Meanwhile, a study by Hariyadi (2019) on tomato drying using 2 mm and 4 mm slices in a tray dryer with hot air temperatures of 40℃, 50℃, 60℃, and 70℃ at an airflow velocity of 2 m/s, concluded that the best result was obtained at a drying temperature of 50℃ with a 4 mm slice thickness.

This study aimed to analyze the temperature distribution and airflow pattern inside a tray dryer during the carrot drying process using Computational Fluid Dynamics (CFD). The results are

Available online:
http://journal.ipb.ac.id/index.php/jtep
DOI: 10.19028/jtep.013.4.329-545

expected to contribute to the improvement of drying system design and operation for better product quality and energy efficiency in the future.

2. Material and Methods

2.1 Research Location and Duration

This study was conducted at the Laboratory of Food and Agricultural Product Processing Engineering, Department of Agricultural and Biosystems Engineering, Faculty of Agricultural Technology, Universitas Andalas, Padang, West Sumatra, Indonesia. The study will be conducted from December 2024 to February 2025.

2.2 Tools and Materials

The equipment used in this study included a tray dryer, digital thermometer, anemometer, digital scale, laptop, exhaust fan, and software such as SolidWorks, ANSYS Fluent, and OriginLab. Fresh carrot (Daucus carota L.) was used, which was cleaned and sliced into round pieces with a thickness of approximately 2 mm.

2.3 Research Method

In this study, we simulated the distribution of temperature and airflow during carrot drying in a tray dryer using Computational Fluid Dynamics (CFD). The simulations were conducted under six conditions with three temperature variations (50°C, 60°C, and 70°C) and two air velocity variations (2 m/s and 3 m/s). The process included material preparation, temperature and air velocity measurements, geometry modeling, CFD simulation, and model validation.

2.4 Material Preparation

Carrots were obtained from traditional markets in Padang, Indonesia. After cleaning, the carrots were sliced into round shapes (±2 mm thickness), air-dried, and arranged on dryer trays.

2.5 Temperature and Air Velocity Measurement

Temperature measurements were performed at five observation points, consisting of three points on the side walls, one point at the plenum, and one point at the outlet. The air velocity was measured at the upper outlet section using an anemometer. For validation, the average measured temperature at these five points and the average measured outlet air velocity were compared with the simulated values at the corresponding locations.

JTEP Jurnal Keteknikan Pertanian,
Vol. 13 No. 4, p 529-545, 2025
P-ISSN 2407-0475 E-ISSN 2338-8439
Available online:
http://journal.ipb.ac.id/index.php/jtep
DOI: 10.19028/jtep.013.4.329-545

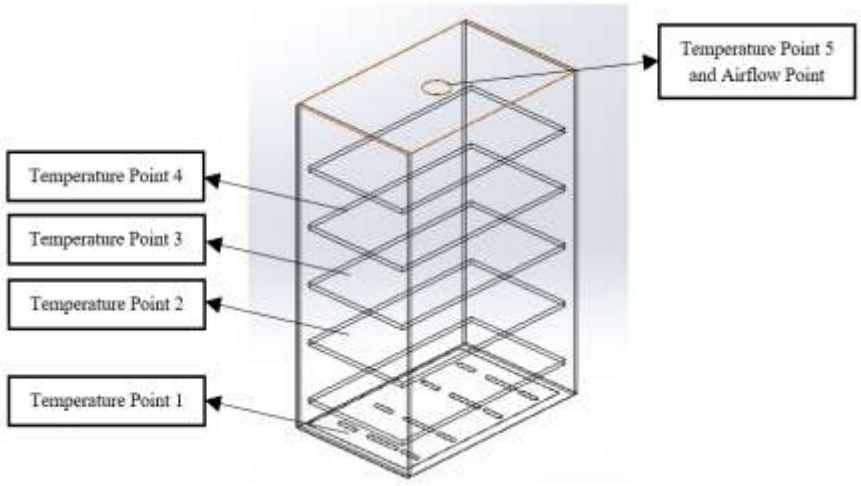

Figure 1. Temperature point, and airflow point.

2.6 Geometry Modeling

The geometry of the tray dryer was created using SolidWorks. The dryer dimensions were 104 cm (length) × 65.01 cm (width) × 143.56 cm (height), with five trays (97.40 cm × 43 cm × 2 cm) spaced 26 cm apart (Figure 2). The airflow inlets, outlets, and walls were clearly defined for the simulation.

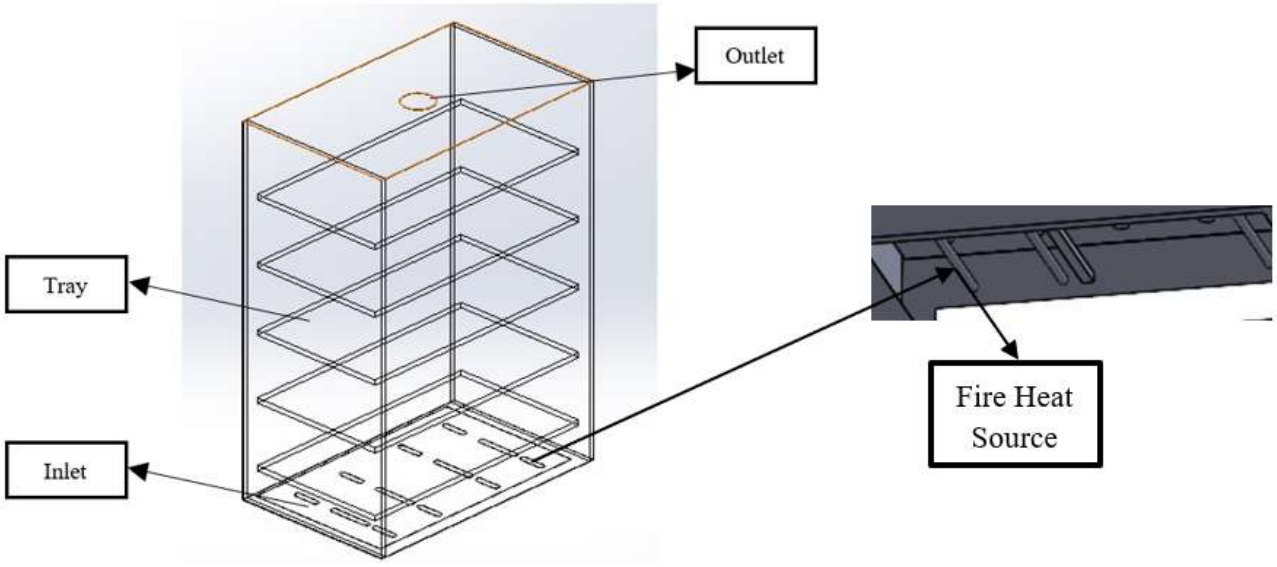

Figure 2. Geometry tray dryer

2.7 CFD Simulation

The CFD simulation consisted of three stages: pre-processing, processing, and post-processing.

- **Pre-processing** included geometry modeling and mesh generation. Meshing was performed using ANSYS with quality criteria (skewness < 0.98 and orthogonal quality > 0.2), resulting in 59,465 nodes and 265,985 elements.

JTEP Jurnal Keteknikan Pertanian,
Vol. 13 No. 4, p 529-545, 2025
P-ISSN 2407-0475 E-ISSN 2338-8439
Available online:
http://journal.ipb.ac.id/index.php/jtep
DOI: 10.19028/jtep.013.4.329-545

- **Processing** involved setting up the simulation in ANSYS Fluent using a steady-state, pressure-based solver, with the k-ω turbulence model and energy equation activated. Air was treated as an incompressible fluid with constant property. The boundary conditions were set at the inlet, outlet, and wall surfaces.

  The governing equations employed in this simulation included the continuity equation, three-dimensional momentum equations, and energy equation. The continuity equation ensures mass conservation within the fluid domain. The momentum equations represent the conservation of linear momentum in the x, y, and z directions, whereas the energy equation describes the mechanism of heat transfer in the fluid flow.

  These equations can be expressed mathematically as follows:

  1. Continuity Equation

     $$\frac{\partial(\rho u)}{\partial x}+\frac{\partial(\rho v)}{\partial y}+\frac{\partial(\rho w)}{\partial z}=0$$

  2. 3-deimensional Momentum Equation

     Momentum in the x direction:

     $$\rho\left[u\frac{\partial u}{\partial x}+v\frac{\partial u}{\partial y}+w\frac{\partial u}{\partial z}\right]=\frac{\partial p}{\partial x}+\mu\left[u\frac{\partial^2 u}{\partial x^2}+v\frac{\partial^2 u}{\partial y^2}+w\frac{\partial^2 u}{\partial z^2}\right]+S_{Mx}$$

     Momentum in the y direction:

     $$\rho\left[u\frac{\partial u}{\partial x}+v\frac{\partial u}{\partial y}+w\frac{\partial u}{\partial z}\right]=\frac{\partial p}{\partial y}+\mu\left[u\frac{\partial^2 u}{\partial x^2}+v\frac{\partial^2 u}{\partial y^2}+w\frac{\partial^2 u}{\partial z^2}\right]+S_{My}$$

     Momentum in the z direction

     $$\rho\left[u\frac{\partial u}{\partial x}+v\frac{\partial u}{\partial y}+w\frac{\partial u}{\partial z}\right]=\frac{\partial p}{\partial z}+\mu\left[u\frac{\partial^2 u}{\partial x^2}+v\frac{\partial^2 u}{\partial y^2}+w\frac{\partial^2 u}{\partial z^2}\right]+S_{Mz}$$

  3. Energy Equation

     $$\rho\left[u\frac{\partial T}{\partial x}+v\frac{\partial T}{\partial y}+w\frac{\partial T}{\partial z}\right]=\rho\left[u\frac{\partial u}{\partial x}+v\frac{\partial u}{\partial y}+w\frac{\partial u}{\partial z}\right]+k\left[\frac{\partial^2 u}{\partial x^2}+\frac{\partial^2 u}{\partial y^2}+\frac{\partial^2 u}{\partial z^2}\right]+S_i$$

- **Post-processing** involved visualizing the simulation results in the form of contour plots, heatmaps, and vector fields to analyze the airflow and temperature distribution. The results were red data using relative error analysis. The percentage error was calculated using the following equation:

  $$Error=\left[\frac{(X\ measured-X\ simulated)}{X\ measured}\right]\times 100\%$$

  Where X represents the measured temperature (℃) or air velocity (m/s). This approach is commonly used in CFD validation studies to quantify the deviation between the simulation and experimental data. Validation was considered acceptable when the error value was less than 10% (Anwar & Panggabean, 2019).

JTEP Jurnal Keteknikan Pertanian,
Vol. 13 No. 4, p 529-545, 2025
P-ISSN 2407-0475 E-ISSN 2338-8439
Available online:
http://journal.ipb.ac.id/index.php/jtep
DOI: 10.19028/jtep.013.4.329-545

The assumptions in this simulation included turbulent flow (Re > 4000) (Wang and Economides, 2009), incompressible air, and stable ambient conditions.

3. Results and Discussion

3.1 Temperature and Air Velocity Measurement

Temperature and air velocity measurements were performed at five observation points inside the tray dryer. The temperature values obtained under various drying conditions are listed in Table 1. These data served as references for validating the CFD simulation model. The air velocities measured at the dryer outlet were 2 m/s and 3 m/s, respectively. The temperature distribution was irregular, particularly in the middle and upper sections of the drying chamber (Figure 3).

Table 1. Measured temperature and air velocity at various points inside the tray dryer.

Treatment	Temperature (℃)	Airflow m/s
Temperature 50℃ and Airflow 2 m/s	46,75	1,95
Temperature 50℃ and Airflow 3 m/s	48,59	2,92
Temperature 60℃ and Airflow 2 m/s	56,66	2
Temperature 60℃ and Airflow 3 m/s	57,68	3,01
Temperature 70℃ dan Airflow 2 m/s	65,17	2,07
Temperature 70℃ dan Airflow 3 m/s	67,06	2,92

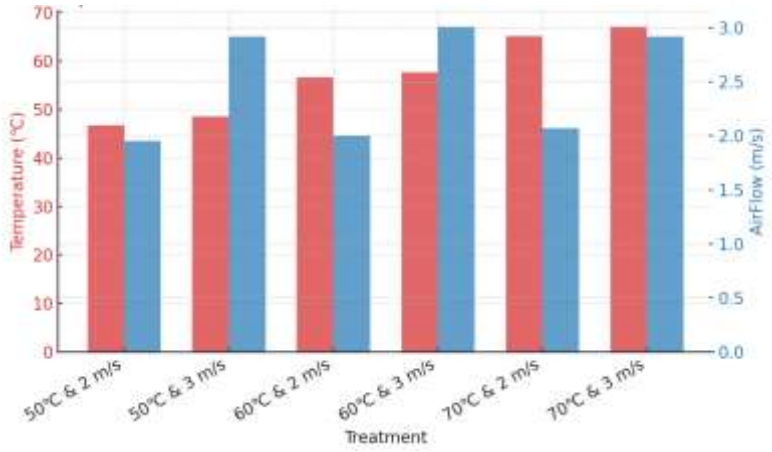

Figure 3. Graph of temperature and air velocity measurements at various points inside the tray dryer.

JTEP Jurnal Keteknikan Pertanian,
Vol. 13 No. 4, p 529-545, 2025
P-ISSN 2407-0475 E-ISSN 2338-8439
Available online:
http://journal.ipb.ac.id/index.php/jtep
DOI: 10.19028/jtep.013.4.329-545

3.2 CFD Simulation Results

CFD simulations were performed under six treatment combinations: temperatures of 50°C, 60°C, and 70°C with air velocities of 2 m/s and 3 m/s. The results were visualized as contour plots and heatmaps to illustrate the airflow and temperature distribution inside the dryer.

3.2.1 Temperature and Airflow Distribution at 50^{0}C and 2m/s

Figure 4 illustrates the simulation results for the tray dryer, showing a non-uniform temperature distribution. This condition indicates suboptimal hot airflow, which contributes to uneven drying and consequently reduces the overall efficiency of drying (Delele et al., 2013).

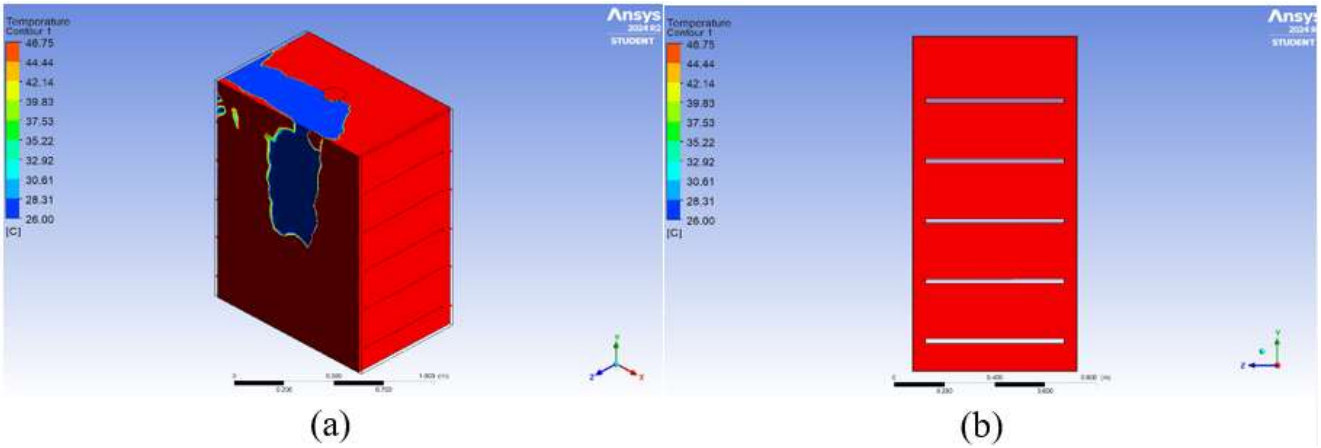

Figure 4. Temperature distribution contour at 50^{0}C and Airflow of 2 m/s in the tray dryer. (a) 3D view (b) Side view

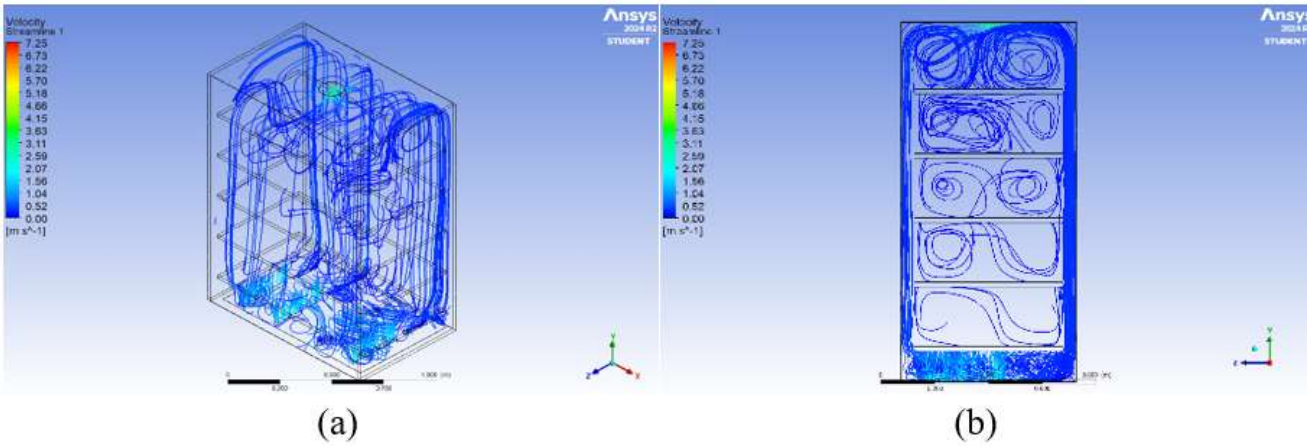

Figure 5. Airflow distribution contour at 2 m/s and 50^{0}C. (a) 3D view (b) Side view.

Figure 5 shows the streamline contour of the airflow with velocities of up to 7.3 m/s. The simulation results show the formation of vortices caused by the internal structure of the tray dryer, with the airflow velocity increasing upward toward the outlet and reaching an average velocity of

JTEP Jurnal Keteknikan Pertanian,
Vol. 13 No. 4, p 529-545, 2025
P-ISSN 2407-0475 E-ISSN 2338-8439
Available online:
http://journal.ipb.ac.id/index.php/jtep
DOI: 10.19028/jtep.013.4.329-545

1.96 m/s. This finding is consistent with the results reported by Cengel and Ghajar (2019), who stated that airflow patterns in enclosed drying systems tend to form vortices and accelerate toward the outlet because of pressure differences.

3.2.2 Temperature and Airflow Distribution at 50^{0}C and 3m/s

Figure 6 illustrates that the temperature distribution within the tray dryer in this study was not uniform, indicating that the hot airflow remained suboptimal even at higher airflow velocities. This finding is consistent with the results reported by Apriansa and Irawan (2024), who observed that increasing the airflow velocity in a tray dryer does not always improve the heat distribution owing to flow recirculation and structural obstructions.

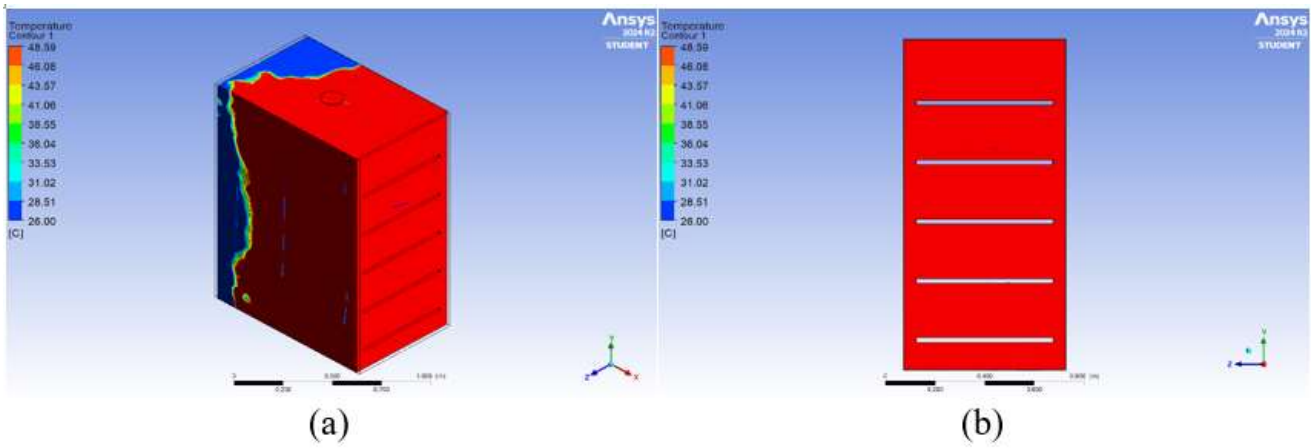

Figure 1. Temperature distribution contour at 50℃ and Airflow of 3 m/s in the Tray Dryer. (a) 3D view (b) Side view.

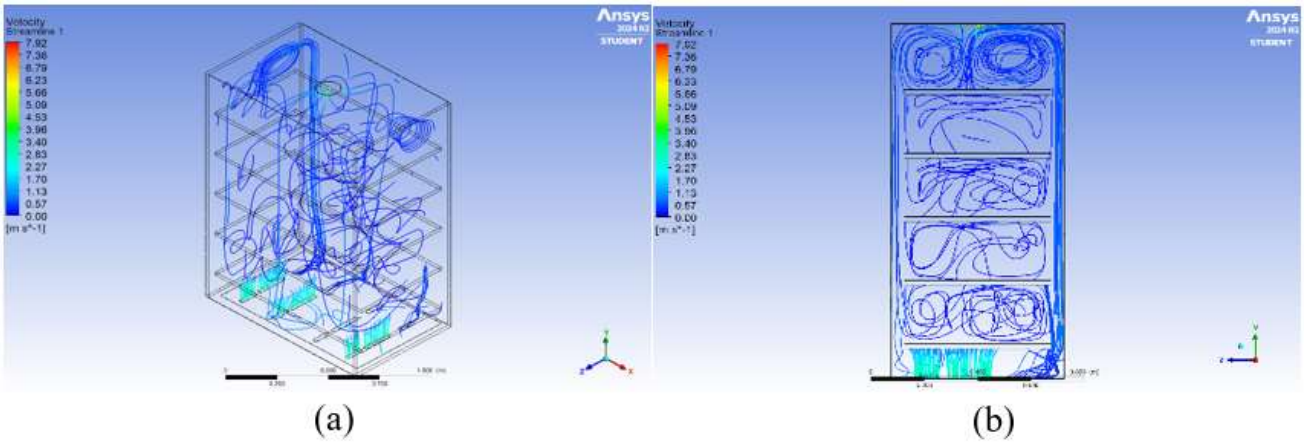

Figure 7. Airflow distribution contour at 3 m/s and 50^{0}C. (a) 3D view (b) Side view.

JTEP Jurnal Keteknikan Pertanian,
Vol. 13 No. 4, p 529-545, 2025
P-ISSN 2407-0475 E-ISSN 2338-8439
Available online:
http://journal.ipb.ac.id/index.php/jtep
DOI: 10.19028/jtep.013.4.329-545

Figure 7 illustrates the airflow streamline patterns observed in this study, showing the formation of vortices and recirculation zones owing to the internal structure of the tray dryer. This result is consistent with the findings of Jading et al. (2018), who reported similar vortex formations in drying systems caused by geometric constraints and flow redirections.

3.2.3 Temperature and Airflow Distribution at 60^{o}C and 2m/s

Figure 8 shows that the temperature distribution in this study was non-uniform, indicating an imbalance in the heat transfer across the tray level. This observation aligns with the results of Has et al. (2021), who found that differences in fluid flow and material properties can cause uneven temperature profiles in tray dryers.

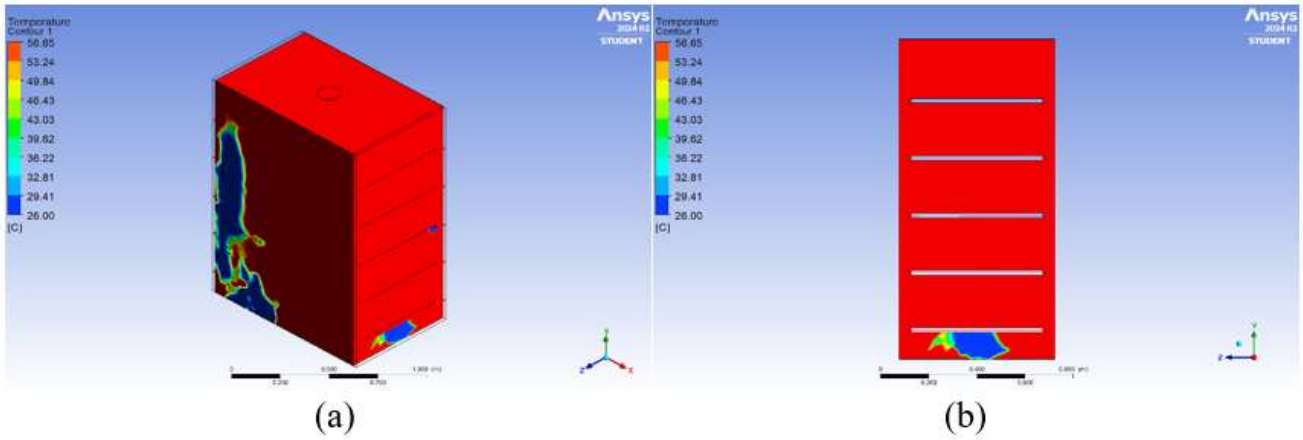

Figure 8. Temperature distribution contour at 60^{0}C and Airflow of 2 m/s in the tray dryer. (a) 3D view (b) Side view.

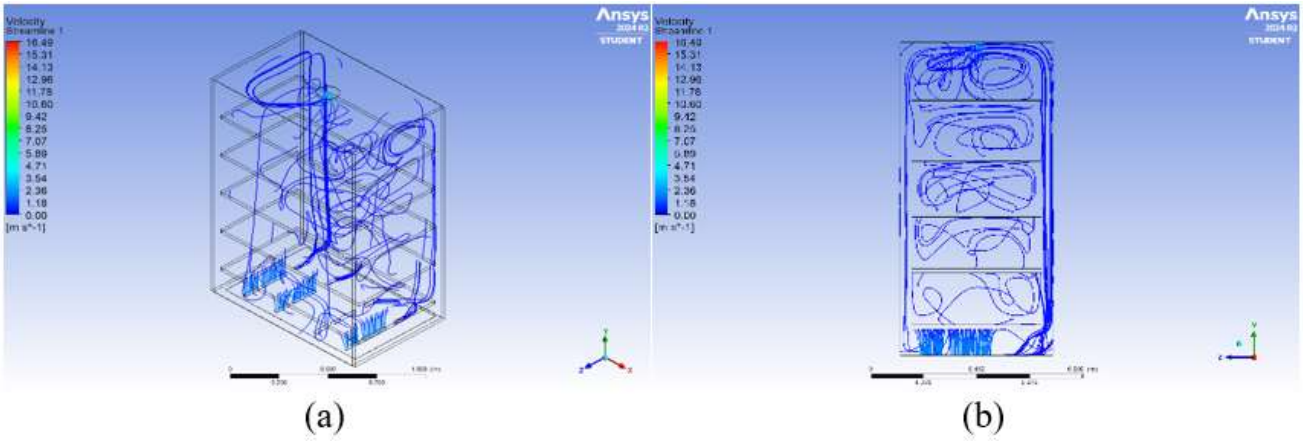

Figure 9. Airflow Distribution contour at 2 m/s and 60^{0}C. (a) 3D view (b) Side view.

JTEP Jurnal Keteknikan Pertanian,
Vol. 13 No. 4, p 529-545, 2025
P-ISSN 2407-0475 E-ISSN 2338-8439
Available online:
http://journal.ipb.ac.id/index.php/jtep
DOI: 10.19028/jtep.013.4.329-545

Figure 9 shows the airflow contour within the tray dryer, showing vortex patterns at each level caused by surface obstructions and changes in the flow direction. The velocity varied and was predominantly represented by blue hues, indicating low-to-moderate airflow (Bangun et al., 2022). These conditions may lead to inconsistencies in the drying process.

3.2.4 Temperature and Airflow Distribution at 60^{o}C and 3m/s

Figure 10 shows the uneven temperature distribution at the front and upper sections of the tray dryer, indicating the presence of cold zones owing to uneven hot airflow. This condition potentially reduces the drying efficiency and uniformity of the product quality (Bangun et al., 2022).

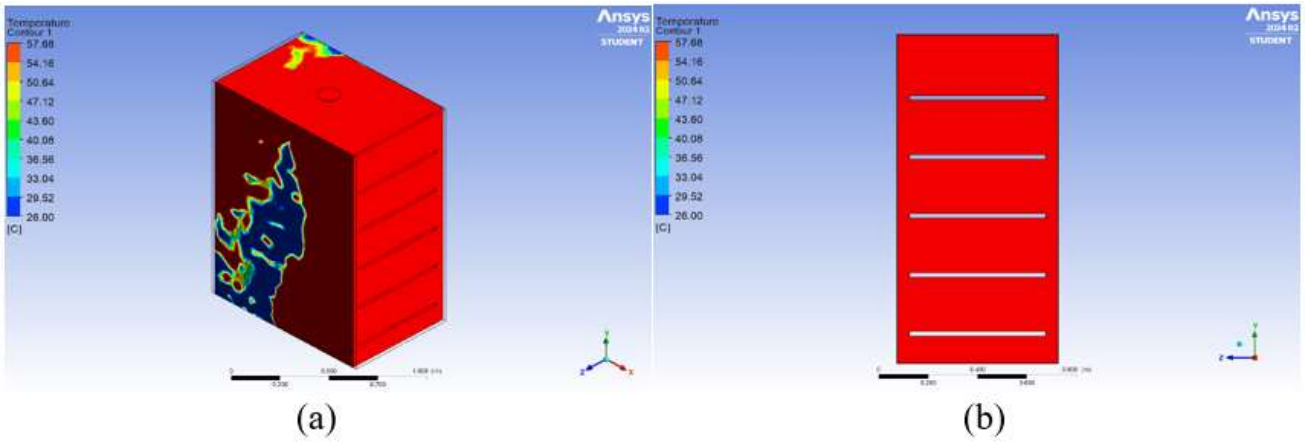

Figure 10. Temperature distribution contour at 60°C and Airflow of 3 m/s in the tray dryer. (a) 3D view (b) Side view.

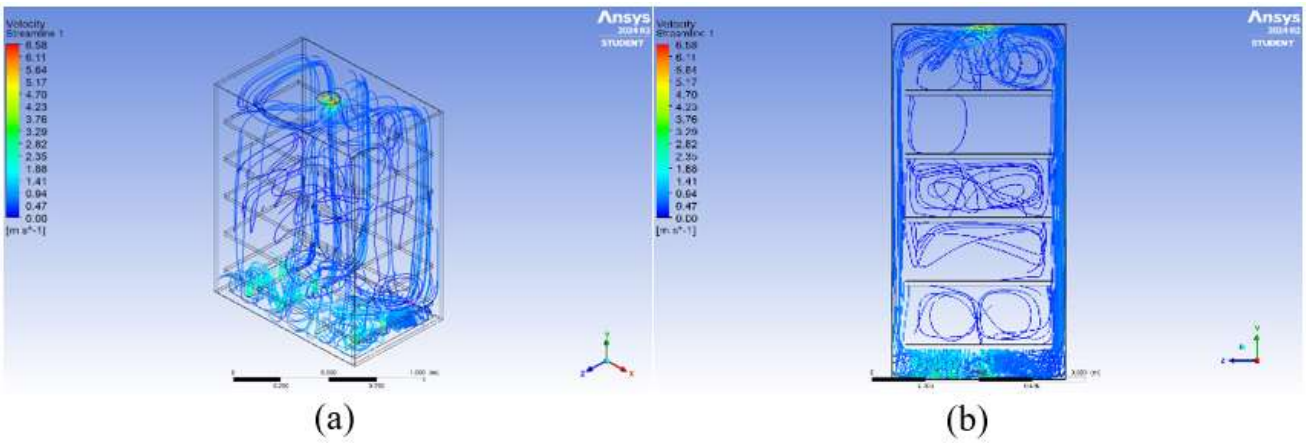

Figure 11. Airflow distribution contour at 3 m/s and 60^{0}c. (a) 3D view (b) Side view.

Figure 11 presents the simulation results of airflow with an input velocity of 3.01 m/s, where the flow spread from top to bottom through the trays, forming circulation and turbulence patterns. This

JTEP Jurnal Keteknikan Pertanian,
Vol. 13 No. 4, p 529-545, 2025
P-ISSN 2407-0475 E-ISSN 2338-8439
Available online:
http://journal.ipb.ac.id/index.php/jtep
DOI: 10.19028/jtep.013.4.329-545

indicates that the airflow distribution remained uneven, particularly in the middle and lower sections of the tray dryer (Bangun et al., 2022).

3.2.5 Temperature and Airflow Distribution at 70^{0}C and 2m/s

Figure 12 indicates that in this study, hot air was concentrated at the bottom section of the tray dryer, leading to noticeable temperature differences between the trays. This finding is similar to that of Has et al. (2021), who reported that lower chamber zones often experience heat accumulation owing to limited vertical airflow.

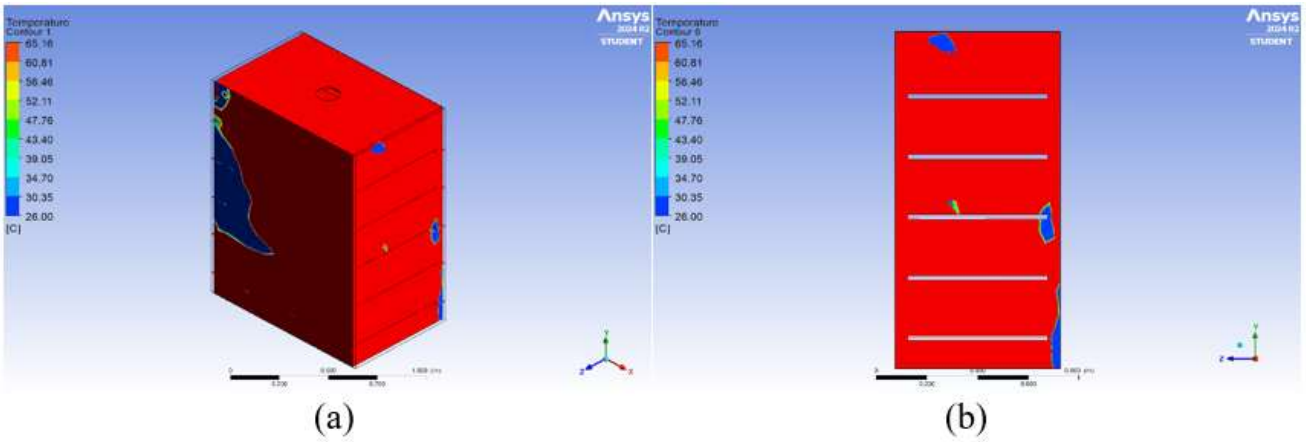

Figure 12. Temperature distribution contour at 70^{0}c and Airflow of 2 m/s in the tray dryer. (a) 3D view (b) Side view.

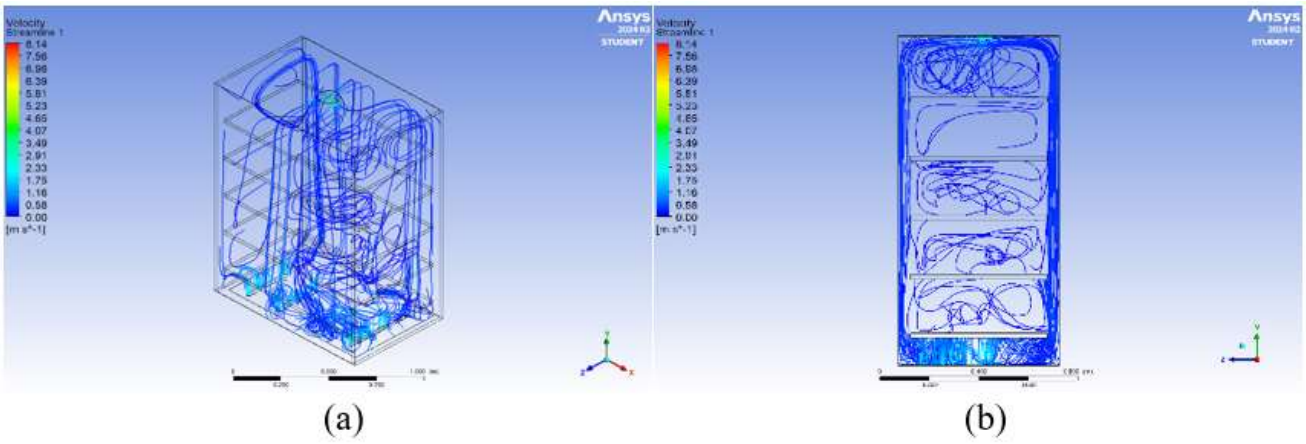

Figure 13. Airflow distribution contour at 2 m/s and 70^{0}c. (a) 3D view (b) Side View.

The airflow in Figure 13 forms a complex streamline pattern, with higher concentrations on the right and lower sides of the tray dryer. In this study, the middle to upper sections were dominated by slow circular airflow patterns, indicating low air-exchange rates in these zones. This condition agrees

JTEP Jurnal Keteknikan Pertanian,
Vol. 13 No. 4, p 529-545, 2025
P-ISSN 2407-0475 E-ISSN 2338-8439
Available online:
http://journal.ipb.ac.id/index.php/jtep
DOI: 10.19028/jtep.013.4.329-545

with the findings of Has et al., (2021), who also observed circular recirculation zones that reduced drying uniformity in the upper tray regions.

3.2.6 Temperature and Airflow Distribution at 70^{0}C and 3m/s

Figure 14 illustrates the high temperatures concentrated at the upper section of the tray dryer, whereas lower temperatures were observed in the lower front and side areas. This indicates that the hot airflow was not evenly distributed, resulting in uneven heat circulation from the heat source within the tray dryer (Bangun et al., 2022).

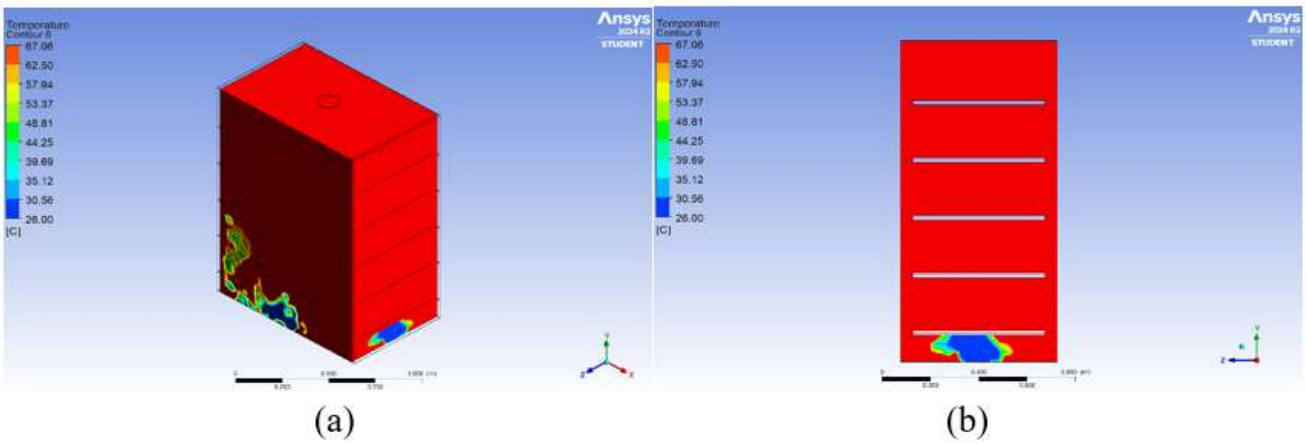

Figure 2. Temperature Distribution Contour at 70^{0}C and Airflow of 3 m/s in the Tray Dryer. (a) 3D view (b) Side View.

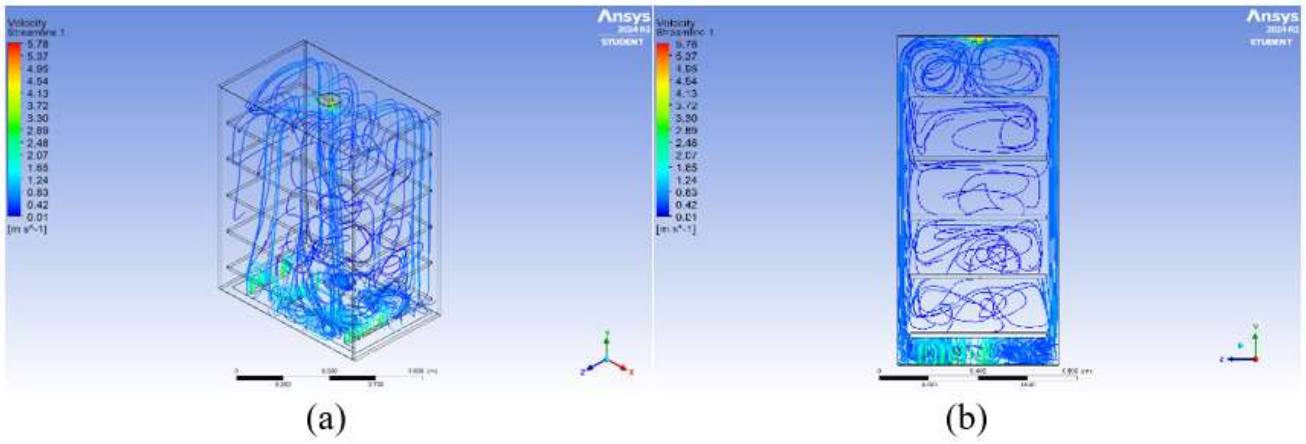

Figure 15. Airflow Distribution Contour at 3 m/s and 70^{0}c. (a) 3D View (b) Side view.

The airflow simulation in Figure 15 shows a distribution that spreads from the top throughout the drying chamber. The airflow distribution in the upper section was found to be relatively adequate in this study. However, airflow to the lower trays remained limited, reducing drying uniformity. This observation corresponds with the theoretical explanation by Cengel and Ghajar (2019), who stated

Available online:
http://journal.ipb.ac.id/index.php/jtep
DOI: 10.19028/jtep.013.4.329-545

that air movement in closed drying systems tends to accelerate toward the outlet, resulting in a weaker flow in the lower regions.

3.3 Model Validation

The model validation was conducted by comparing the average measured values at the designated measurement points with the simulated values at the corresponding locations in the CFD model. The discrepancy reported in this study represents the model deviation relative to the experimental measurements, which was calculated as a percentage of the relative error. This value reflects the accuracy of the CFD model but does not indicate airflow or temperature uniformity, as uniformity should be evaluated using statistical parameters such as the standard deviation or coefficient of variation, which were not analyzed in this study. Therefore, the deviations obtained (1.41–3.82% for temperature and 0.5–2.41% for air velocity) confirm good agreement between the model and experiment but cannot be interpreted as indicators of uniform distribution within the tray dryer (Anwar and Panggabean, 2019).

Table 2. Comparison of the measured and simulated temperature values.

Treatment	Temperature ℃		*Error* (%)
	Measured	Simulated	
Temperature 50℃ dan Airflow 2 m/s	46,75	45,73	2,18
Temperature 50℃ dan Airflow 3 m/s	48,59	47,25	2,78
Temperature 60℃ dan Airflow 2 m/s	56,66	54,49	3,83
Temperature 60℃ dan Airflow 3 m/s	57,68	56,15	2,65
Temperature 70℃ dan Airflow 2 m/s	65,17	63,89	1,96
Temperature 70℃ dan Airflow 3 m/s	67,06	66,11	1,41

Table 3. Comparison of the measured and simulated air velocity values.

Treatment	Airflow (m/s)		*Error* (%)
	Measured	Simulated	
Temperature 50℃ dan Airflow 2 m/s	1,95	1,97	1,03
Temperature 50℃ dan Airflow 3 m/s	2,92	2,95	1,03
Temperature 60℃ dan Airflow 2 m/s	2	2,01	0,5

Continue

JTEP Jurnal Keteknikan Pertanian,
Vol. 13 No. 4, p 529-545, 2025
P-ISSN 2407-0475 E-ISSN 2338-8439
Available online:
http://journal.ipb.ac.id/index.php/jtep
DOI: 10.19028/jtep.013.4.329-545

Continue

Treatment	Airflow (m/s)		*Error (%)*
	Measured	Simulated	
Temperature 60℃ dan Airflow 3 m/s	3,01	3,04	0,99
Temperature 70℃ dan Airflow 2 m/s	2,07	2,02	2,41
Temperature 70℃ dan Airflow 3 m/s	2,92	2,89	1,03

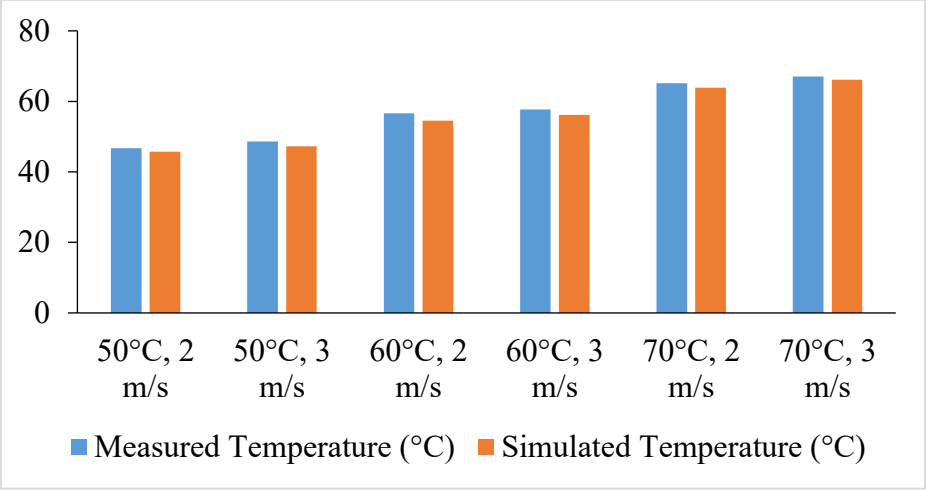

Figure 16. Comparison graph of measured and simulated temperature value.

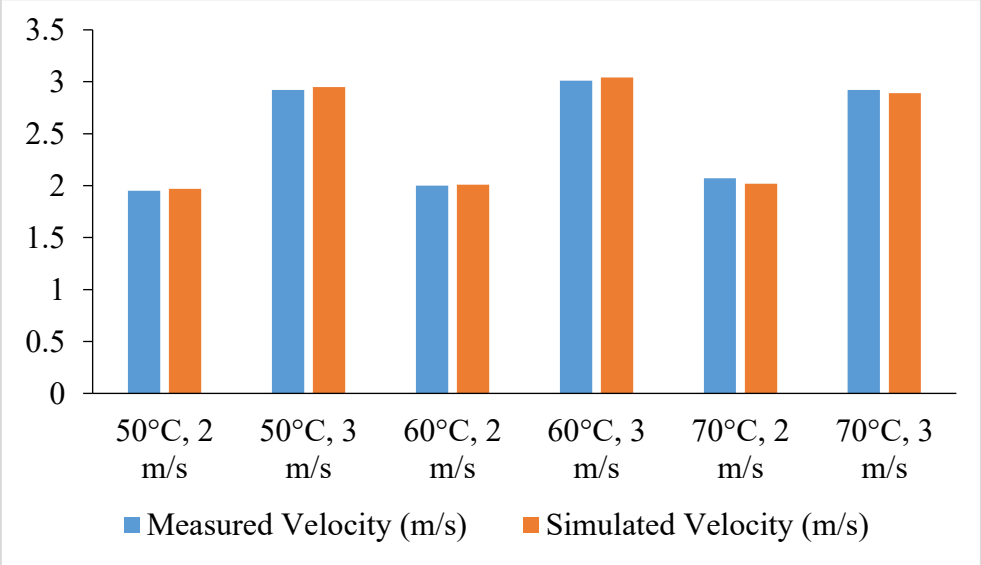

Figure 17. Comparison graph of measured and simulated air velocity values.

Available online:
http://journal.ipb.ac.id/index.php/jtep
DOI: 10.19028/jtep.013.4.329-545

4. Conclusion

Different irradiation durations significantly affected the oxidative stability and sensory quality of avocado mayonnaise. Increases in the peroxide value and free fatty acid content indicate the susceptibility of the product to oxidative deterioration. Significant sensory changes also occurred, as evidenced by a drop in the color score from 6.07 (liked) to 3.47 (disliked) and an aroma score from 6.20 (liked) to 3.67 (neutral). The results of this study confirm that sensory and oxidative parameters are closely linked through photooxidation. Based on these findings, it is recommended that the production and storage of avocado-based mayonnaise be conducted with minimal light exposure and not exceed 24 h (L2), as at this duration the FFA value still meets the Indonesian National Standard (SNI) and the sensory quality remains acceptable. However, the moisture content exceeding the SNI standard suggests that this product naturally possesses characteristics that differ from those of conventional mayonnaise. Therefore, formulation adjustments, such as reducing the proportion of avocado, increasing the oil content, or using stabilizing agents, should be considered if compliance with mayonnaise standards is necessary. In addition, the use of light-impermeable packaging or packaging with UV protection is important for maintaining oxidative stability and sensory quality during distribution and storage. By implementing these strategies, nutritional quality, emulsion stability, and consumer acceptance of avocado mayonnaise can be optimally maintained in the future. The simulation of temperature and airflow distribution in carrot drying using a tray dryer and Computational Fluid Dynamics (CFD) revealed that airflow and temperature were not evenly distributed across all tray levels. Higher air velocities contributed to more uniform temperature profiles and improved the heat transfer. Among the six treatment conditions, a temperature of 70°C and air velocity of 3 m/s produced the most optimal drying uniformity based on the CFD visualization results. The airflow and temperature contours under these conditions appeared more evenly distributed than those under other treatments. Quantitatively, this can be confirmed by comparing the standard deviation values of the temperature and air velocity, where the lowest deviations indicate the most uniform drying conditions. However, future work should include a quantitative analysis using the standard deviation or coefficient of variation to numerically evaluate the temperature and airflow uniformity among the treatments.

5. References

Al-kindi, H., Purwanto, Y. A., & Wulandani, D. (2015). Analisis cfd aliran udara panas pada pengering tipe rak dengan sumber energi gas buang distibtuion analysis hot air flow of rack type dryer with energy source from exhaust gas using Computational Fluid Dynamics (CFD). Jurnal Keteknikan Pertanian, 3(1), 9–16.

Available online:
http://journal.ipb.ac.id/index.php/jtep
DOI: 10.19028/jtep.013.4.329-545

Anwar, C., & Panggabean, S. (2019). Kajian distribusi suhu dan aliran udara pada alat pengering chips temulawak tipe rak menggunakan simulasi Computational Fluid Dynamics (CFD). Jurnal Rekayasa Pangan Dan Pertanian, 7(4), 291–298.

Apriansa, F., & Irawan, R. (2024). Optimization of dehumidification air flow distribution in temulawak tray dryer with Computational Fluid Dynamics (CFD). Jurnal Asiimetrik: Jurnal Ilmiah Rekayasa Dan Inovasi, 6(2), 327–340. https://doi.org/10.35814/asiimetrik.v6i2.6664

Bangun, R., Pemotong, A., Dengan, U. O., Ulir, P., Pegas, D. A. N., & Motor, B. (2022). Jurnal Inovasi Mesin. 4(1), 1–12.

Daza-Gómez, M. A. M., Gómez Velasco, C. A., Gómez Daza, J. C., & Ratkovich, N. (2022). 3D computational fluid dynamics analysis of a convective drying chamber. Processes, 10(12). https://doi.org/10.3390/pr10122721

Delele, M. A., Ngcobo, M. E. K., Getahun, S. T., Chen, L., Mellmann, J., & Linus, U. (2013). Postharvest biology and technology studying airflow and heat transfer characteristics of a horticultural produce packaging system using a 3-d cfd model . part ii : effect of package design. Postharvest Biology and Technology, 86, 546–555. https://doi.org/10.1016/j.postharvbio.2013.08.015

Hariyadi, T. (2019). Aplikasi metoda foam-mat drying pada proses pengeringan tomat menggunakan tray dryer. Industrial Research Workshop and National Seminar, 250–257.

Has, R. A., Purnamasari, I., & Fadarina, F. (2021). Efisiensi thermal alat pengering tipe tray untuk pengeringan pulp campuran tandan kosong kelapa sawit dan pelepah pisang. Jurnal Pendidikan Dan Teknologi Indonesia, 1(12), 511–519. https://doi.org/10.52436/1.jpti.137

Histifarina, D., Musaddad, D., & Murtiningsih, E. (2004). Teknik pengeringan dalam oven untuk irisan wortel kering bermutu. Jurnal Hortikultura, 14(2), 107–112.

Jading, A., Bintoro, N., Sutiarso, L., & Wahyu Karyadi, J. N. (2018). Temperature and air velocity simulation on sago starch pneumatic conveying recirculated dryer using ansys fluent. Agritech, 38(1), 88. https://doi.org/10.22146/agritech.18251

Kereh, R. L., Riza, A., & Tanujaya, H. (2022). Analisis karakteristik pengering sampah organik tipe tray dryer dengan pendekatan cfd. Jurnal Ilmiah Indonesia, 7(7), 9804–9815.

Saidi, I. A., & Wulandari, F. E. (2019). Pengeringan sayuran dan buah-buahan. in pengeringan sayuran dan buah -buahan.

Tayyeb, N., Arezou, J., Mohammad Hossein, K., & Mortaza, A. (2013). CFD simulation and optimization of factors affecting the performance of a fluidized bed dryer. Iranian Journal of Chemistry and Chemical Engineering, 32(4), 81–92.

Triyastuti, M. S., Finarianingrum, T., & Octaviani, T. (2018). Validasi model pada pengeringan batch pada wortel. Jurnal Teknik: Media Pengembangan Ilmu Dan Aplikasi Teknik, 17(1), 48. https://doi.org/10.26874/jt.vol17no1.55

Wang, X., & Economides, M. (2009). Uploaded by: Ebooks Chemical Engineering.

JTEP Jurnal Keteknikan Pertanian,
Vol. 13 No. 4, p 529-545, 2025
P-ISSN 2407-0475 E-ISSN 2338-8439

Available online:
http://journal.ipb.ac.id/index.php/jtep
DOI: 10.19028/jtep.013.4.329-545

Yunus A. Cengel, & Ghajar, A. J. (2019). Heat and mass transfer. In Sustainability (Switzerland).Vol 11(1).http://scioteca.caf.com/bitstream/handle/123456789/1091/RED2017Eng8ene.pdf?sequence=12&isAllowed=y%0Ahttp://dx.doi.org/10.1016/j.regsciurbeco.2008.06.005%0Ahttps://www.researchgate.net/publication/305320484_Sistem_pembetungan_terpusat_strategi_melestari